SUPPORTING INFORMATION

Wafer scale fabrication of porous three dimensional plasmonic metamaterials for the visible: chiral and beyond

Johnson Haobijam Singh,*[a] Greshma Nair, [b] Arijit Ghosh, [c] Ambarish Ghosh [abc]**

[a] *Department of Physics Indian Institute of Science, Bangalore, 560012, India;*
[b] *Centre for Nano Science and Engineering, Indian Institute of Science, Bangalore, 560012, India*
[c] *Department of Electrical Communications Engineering, Indian Institute of Science, Bangalore, 560012, India*

* *Email: johnsonthonga196@gmail.com*
** *Email: ambarish@ece.iisc.ernet.in*

Experimental Section:

Fabrication*:* The SiO_2 helical films were fabricated in a commercial Glancing Angle Deposition System equipped with electron beam evaporation and thermal evaporation. We have also experimented with other dielectrics, such as MgF_2 and TiO_2, and although the results differ in details, the general conclusions of this manuscript remain the same. A glass substrate was placed at 84° angle to the source of incoming vapour and was rotated (clockwise or counter clockwise) at a speed of 0.05 – 0.1 rpm for film evaporation rates of 0.1 – 0.2 nm/second. The choice of the tilt angle and the rotation speed was based on the particular design of the helix, whose details are well described in the literature pertaining to glancing angle deposition. Subsequently, the substrate was tilted so that the normal to the substrate was at 5° to the incoming vapour and rotated at ~ 1.5 rpm while 1 – 20 nm of Ag or Au was evaporated. To prepare the isotropic solution of the helices, a known size of the film (1cm × 1cm) was sonicated in 400 µl of DI water (millipore) for about 1 minute. The solution (~ 250 µl) was transferred to a glass cuvette (5mm × 5mm) for the measurements. For the heating experiments, the glass substrates containing the chiro-plasmonic helical films were placed on a hot plate set at a particular temperature for about 5-30 minutes. During this time, the samples were covered such as to prevent any convective air flow. The CD measurements were performed after the samples were allowed to cool down to room temperature.

Characterization: The films were optically characterized in a system comprising of a lamp and a monochromator (Horiba Yvon), photoelastic modulator (Hinds Instruments) and photodiode (Thorlabs). Light of a particular wavelength was modulated between left and right circularly polarized states at 42 KHz and transmitted through the substrate onto the photodetector. The length of the cables and the load resistance across the photodiode was kept sufficiently low to ensure the temporal response of the detector to be faster than 150 KHz. The circular dichroism signal was measured though a lock-in amplifier (Signal Recovery) through standard phase locked detection techniques. We measured the absorbance of the sample using a spectrometer (Ocean Optics), which was used in estimating the anisotropy factor.

Contributions from linear dichroism:

To estimate the contribution from linear dichroism of the samples to the measurement of circular dichroism, we performed an experiment where the light was incident normal to the substrate and the CD was measured for various rotation angles of the substrate around the normal direction. There was a minor variation in the CD signal as a function of the rotation angle, which proved that the contribution from linear dichroism was not a dominant factor.

The results for various rotation angles (in degrees) are shown below, along with the peak position and the magnitude of ΔA/A at the peak position in a tabular format.

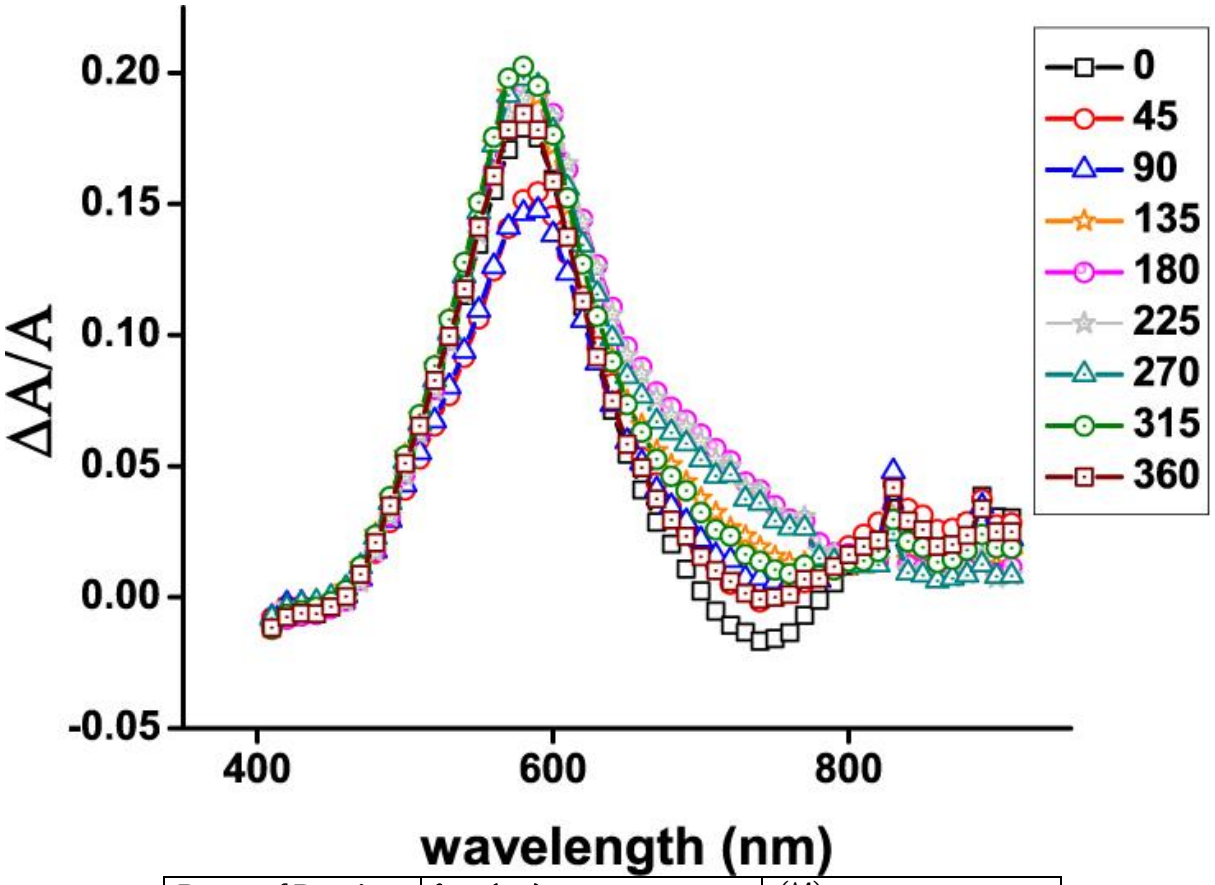

Degree of Rotation	λ_{peak} (nm)	$\left(\frac{\Delta A}{A}\right)_{peak}$
0	580	0.17909
45	590	0.15477
90	590	0.14767
135	580	0.19498
180	590	0.19502
225	590	0.19503
270	580	0.19793
315	580	0.20268
360	580	0.18451

Chiro-optical spectra for an isotropic collection of metal coated helices, along with the results for a film:

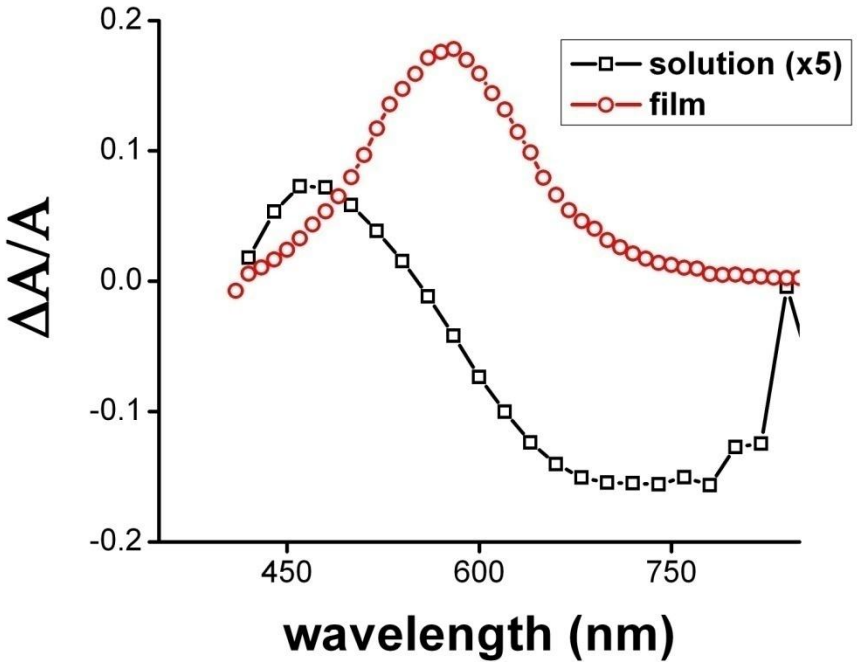

Details of the Numerical Calculation:

The calculations are based on methods described in references 1, 2 and 3. We assume a system of metal nanoparticles (of radius *a*) on a single helix (two turns) of radius 50 nm and pitch 150 nm. We assume the surrounding medium to have a refractive index 1. We have neglected the presence of the helical template made of SiO_2, which contributes negligible CD response in the spectral range of our interest and have confirmed this assumption experimentally.

Each asymmetric nanoparticle is described by a 3 × 3 polarizability tensor which can be oriented in a random direction. In the presence of an external light source incident along the axis of the helix, the total field experienced by a single dipole is the sum of external electrical field and the induced field due to all other dipoles. The self consistent response for the system of dipoles is therefore obtained by solving a set of coupled linear equations, which in turn can be used to calculate the extinction (or absorption) cross sections for left (LCP) and right (RCP) circularly polarised incident light. For the geometries considered here, the difference between absorption and extinction cross-sections were found to negligible (implying very little scattering, as was confirmed from experiments). We have used the same definition for circular dichroism (extinction) as given in ref. 1:

$$\sigma_{CD} = \sigma_L - \sigma_R \qquad (1)$$

The anisotropy factor g is defined as

$$g = \frac{\sigma_{CD}}{\sigma_{avg}} \qquad (2)$$

where,

$$\sigma_{avg} = (\sigma_L + \sigma_R)/2 \qquad (3)$$

The couple dipole equations used in our model are summarised below:

For a system of interaction dipoles, the dipole moment experienced by the i[th] particle is

$$\overrightarrow{p_i} = \alpha_i \cdot \overrightarrow{E_{tot,i}} \qquad (4)$$

where $\overrightarrow{E_{tot,i}}$ is the total field experienced by the i[th] dipole, given by,

$$\overrightarrow{E_{tot,i}} = \overrightarrow{E_{ext,i}} + \overrightarrow{E_{ind,i}} \qquad (5)$$

where $\overrightarrow{E_{ext,i}}$ is the incident field on the i[th] dipole and $\overrightarrow{E_{ind,i}}$ is the induced field on the i[th] dipole by all other dipoles and is given as:

$$\overrightarrow{E_{ind,i}} = \sum_{i \neq j} \left[\frac{3(\overrightarrow{p_i} \cdot \overrightarrow{n_{ij}}) \cdot \overrightarrow{n_{ij}} - \overrightarrow{p_i}}{r_{ij}^3} \left(1 - i\vec{k}.\overrightarrow{r_{ij}}\right) + \left(\frac{\varepsilon_m}{c^2}\,\omega^2\right) \frac{(\overrightarrow{p_i} \cdot \overrightarrow{n_{ij}}) \cdot \overrightarrow{n_{ij}} - \overrightarrow{p_i}}{r_{ij}} \right] e^{i\vec{k}.\overrightarrow{r_{ij}}} \qquad (6)$$

where ε_m is the dielectric constant of the surrounding medium, $k = \sqrt{\varepsilon_m}\, k_o$, with $k_o = \frac{2\pi}{\lambda}$ is the wave number in vacuum, $\overrightarrow{r_{ij}} = \overrightarrow{r_j} - \overrightarrow{r_i}$; $\overrightarrow{r_i}$ is the position vector of the i[th] dipole, $\overrightarrow{n_{ij}} = \frac{\overrightarrow{r_{ij}}}{r_{ij}}$ is the unit vector pointing from i[th] particle to j[th] particle.

For the definition of polarizability, α for a non spherical particle we used the expression from literature[4], given by:

$$\alpha_i = \frac{V}{\left(L_i + \frac{\varepsilon_m}{\varepsilon - \varepsilon_m}\right) + A\varepsilon_m X^2 + B\varepsilon_m^2 X^4 - i\left(\frac{4\pi^2 \varepsilon_m^{\frac{3}{2}}}{3}\right)\frac{V}{\lambda^3}} \qquad (7)$$

where, V is the volume of the nanoparticle

$X = \frac{2\pi a_i}{\lambda}$ is the size parameter and a_i is the semi axis of the nanoparticle

L_i is the geometrical factor describing the aspect ratio of the particles.

For A and B in equation 7, we used the same definition as reported in reference 4.

To account for the random orientation of the particles we used the standard rotation matrix defined with respect to the 3 Euler angles ϕ, θ, ψ, obtained from a uniformly distributed sequence of random numbers between 0 and 2π.

$$R = \begin{bmatrix} \cos\phi\cos\psi - \sin\phi\cos\theta\sin\psi & -\cos\phi\sin\psi - \sin\phi\cos\theta\cos\psi & \sin\phi\sin\theta \\ \sin\phi\cos\psi + \cos\phi\cos\theta\sin\psi & -\sin\phi\sin\psi + \cos\phi\cos\theta\cos\psi & -\cos\phi\sin\theta \\ \sin\theta\sin\psi & \sin\theta\cos\psi & \cos\theta \end{bmatrix} \qquad (8)$$

The new polarizability α' is given by,

$$\alpha' = R^{-1}\alpha\, R. \qquad (9)$$

Using equations from (4) to (8) it is possible to calculate the dipole moment $\vec{p}_i(s)$. The corresponding absorption and extinction cross sections for left and right circularly polarized light can be obtained using the equations below:

$$\sigma_{abs,(L/R)} = 4\pi k\,.\,\mathrm{Im}\left[\sum_i \frac{\vec{p}_{i,(L/R)}^{\,*} \cdot \vec{p}_{i,(L/R)}}{\alpha_i^{\,*}}\right]$$

$$\sigma_{ext,(L/R)} = 4\pi k\,.\,\mathrm{Im}\left[\sum_i \vec{E}_{ext,i(L/R)}^{\,*} \cdot \vec{p}_{i,(L/R)}\right]$$

***Simulation parameters**:* The parameters chosen in the simulations for the case shown in Figure 2D were a = 5 nm, r = 23 nm, δa = 0 nm, 2.5 nm, δr = 0 nm, 2.5 nm. The simulation parameters chosen for the case shown in Figure 3D were a = 14 nm and r = 21 nm. In both cases, we assumed the particles to be Au. For the figure shown under "Thickness dependence red shift of the chiro-optical response" we used the following parameters: helix radius = 70 nm, pitch = 180 nm, spacing r = 31 nm for both a = 5 nm and 10 nm.

Thickness dependent red shift of the chiro-optical response:

SEM images show the metal islands for the unheated samples can be highly non-spherical, which upon heating, become more spherical of approximately the same volume. Imaging these islands such as to obtain detailed geometrical information is very difficult, due to unavoidable charging issues of the underlying dielectric template in the SEM.

To understand how the average geometrical properties of the metallic islands varied with film thickness, we deposited films of 1.5, 3 and 20 nm of Ag on a Si wafer at a glancing angle of 5°, thus obtaining identical conditions at which the metal films were evaporated on the dielectric helices at almost-normal incidence. We believe that the resultant islands had very similar geometrical properties to what has been deposited on the helical templates. The films showed an increase of the average size, and more importantly, the average non-sphericity of the metal particles as a function of increasing film thickness, as shown in the following figure.

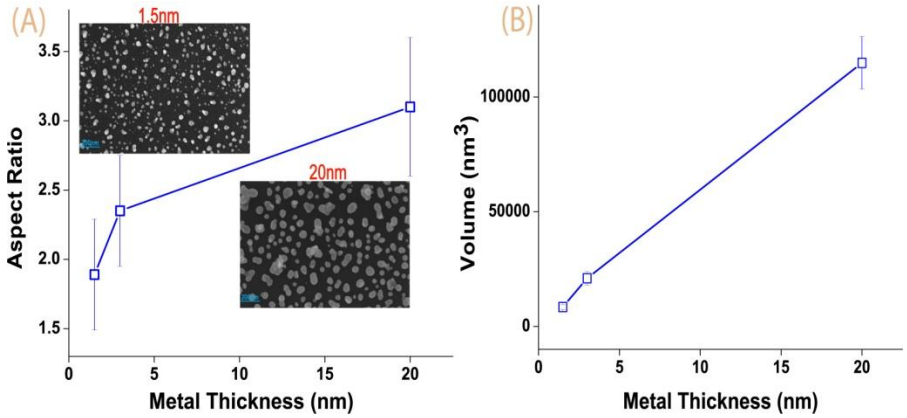

Changing the film thickness caused large differences in size, shape, spacing and number of particles, all of which could affect the chiroptical response of the samples. Coming up with a theoretical model, taking into account all these parameters, is an enormous challenge and is not within the scope of the present manuscript. Accordingly, we investigated, which of these parameters may be the most likely cause behind the large thickness dependent red-shift in the chiro-optical spectra of the present system. We performed simulations on randomly oriented Au nanoparticles with three different ellipticities 0, 2 and 2.5. Two sizes (equivalent radius 5 nm and 10 nm) were considered and the spacing between the nanoparticles was kept constant (r/a > 3) for the particular size. The results are shown in the figure below.

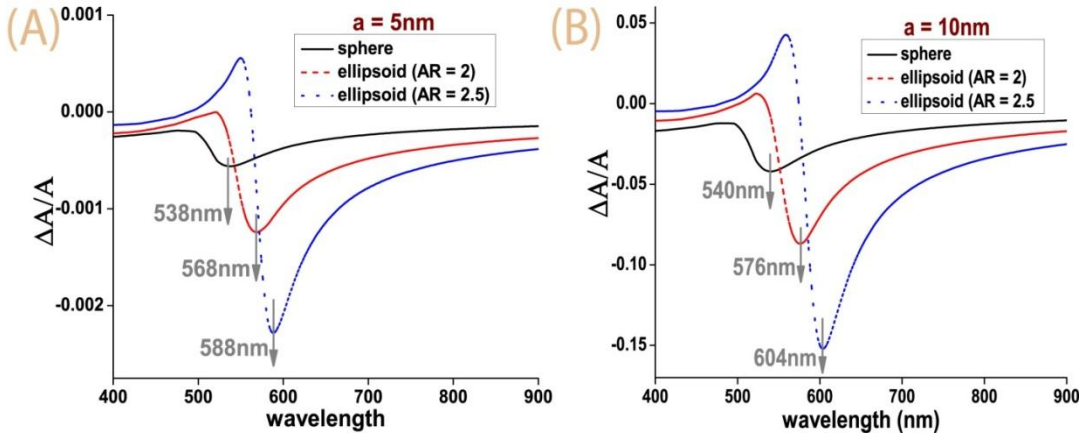

The simulations show a large red shift of the chiro-optical response as the ellipticity was increased, and this effect was stronger in larger particles. The effect of increased thickness in the present system resulted in larger size, as well as ellipticity of the metallic islands, and thus provides explanation on how increase of metallic thickness may result in red shift of the chiro-optical spectrum.

References for Supporting Information:

1. Fan, Z. & Govorov, A. O., *Nano Letters*, 2010, **10,** 2580-2587.
2. Fan, Z. & Govorov, A. O., *J. Phys. Chem. C*, 2011, **115,** 13254–13261.
3. Guerrero-Martínez, A. et al., *Angewandte Chemie International Edition*, 2011, **50,** 5499-5503.
4. Kuwata, Hitoshi, et al., *Applied physics letters*, 2003, **83.22**, 4625-4627.